HHS Public Access

Author manuscript

Dev Neurosci. Author manuscript; available in PMC 2017 September 14.

Published in final edited form as:

Dev Neurosci. 2016 ; 38(4): 277–294. doi:10.1159/000448585.

Hypothermia and rewarming activate a macroglial unfolded protein response independent of hypoxic-ischemic brain injury in neonatal piglets

Jennifer K. Lee, MD[a], **Bing Wang, MD, PhD**[a], **Michael Reyes, BA**[a], **Jillian S. Armstrong, BS**[a], **Ewa Kulikowicz, MS**[a], **Polan T. Santos, MD**[a], **Jeong-Hoo Lee, BS**[a], **Raymond C. Koehler, PhD**[a], and **Lee J. Martin, PhD**[b]

[a]Department of Anesthesiology and Critical Care Medicine, Johns Hopkins University, Baltimore, Maryland [b]Department of Pathology, Division of Neuropathology, Johns Hopkins University, Baltimore, Maryland

Abstract

Therapeutic hypothermia provides incomplete neuroprotection after hypoxia-ischemia (HI)-induced brain injury in neonates. We previously showed that cortical neuron and white matter apoptosis are promoted by hypothermia and early rewarming in a piglet model of HI. The unfolded protein response (UPR) may be one of the potential mediators of this cell death. Here, neonatal piglets underwent HI or sham surgery followed by 29 hours of normothermia, 2 hours of normothermia+27 hours of hypothermia or 18 hours of hypothermia+rewarming. Piglets recovered for 29 hours. Immunohistochemistry for endoplasmic reticulum to nucleus signaling-1 protein (ERN1), a marker of UPR activation, was used to determine the ratios of ERN1+ macroglia and neurons in the motor subcortical white matter and cerebral cortex. The ERN1+ macroglia were immunophenotyped as oligodendrocytes and astrocytes by immunofluorescent co-labeling. Temperature (p=0.046) and HI (p<0.001) independently affected the ratio of ERN1+ macroglia. In sham piglets, sustained hypothermia (p=0.011) and rewarming (p=0.004) increased the ERN1+ macroglia ratio above that in normothermia. HI prior to hypothermia diminished the UPR. Ratios of ERN1+ macroglia correlated to white matter apoptotic profile counts in shams (r=0.472; p=0.026), thereby associating UPR activation with white matter apoptosis during hypothermia and rewarming. Accordingly, macroglial cell counts decreased in shams that received sustained hypothermia (p=0.009) or rewarming (p=0.007) compared to those in normothermic shams. HI prior to hypothermia neutralized the macroglial cell loss. Neither HI nor temperature affected ERN1+ neuron ratios. In summary, delayed hypothermia and rewarming activate the macroglial UPR, which is associated with white matter apoptosis. HI may decrease the macroglial endoplasmic reticulum stress response after hypothermia and rewarming.

Corresponding Author: Jennifer K. Lee, MD, Department of Anesthesiology and Critical Care Medicine, Johns Hopkins Hospital, Charlotte R. Bloomberg Children's Center, 1800 Orleans Street, Room 6321, Baltimore, MD 21287, Phone: 410-955-6412, FAX: 410-502-5312, jklee@jhmi.edu.

None of the authors has a conflict of interest associated with this research.

Keywords

neonate; brain injury; ischemia; endoplasmic reticulum; hypothermia; apoptosis

INTRODUCTION

Therapeutic hypothermia reduces the risk of death and neurologic disability in neonatal hypoxic-ischemic encephalopathy (HIE). [1] However, approximately half of survivors have persistent neurodevelopmental disabilities despite receiving hypothermia. [1, 2] We theorize that adverse effects from delaying the induction of hypothermia [3] and rewarming [4, 5] may be partially responsible for these neurologic impairments. We previously demonstrated that rewarming increases cortical neuronal apoptosis and caspase-3 cleavage after hypoxia-ischemia (HI) in a piglet model. [4] Hypothermia and rewarming also promote glial apoptosis in the white matter, an effect that may be independent of HI in some brain regions. [5] Cortical and white matter injuries on MRI predict neurodevelopmental and motor impairments in survivors of HIE. [6, 7] Thus, there is need to define the mechanisms through which apoptotic cascades are activated after HI, hypothermia, and rewarming; to clarify targets for adjuvant therapies; and to minimize off-target effects from hypothermia and rewarming.

HI, hypothermia, and rewarming are cellular stressors that alter cellular metabolism, protein synthesis, quality control, and survival. [4, 5, 8-10] These events can be upstream signals for cell death. Endoplasmic reticulum (ER) stress is involved in the cellular heat-shock response [11] and may also mediate cellular injury during hypothermia and rewarming. ER stress activates the canonical unfolded protein response (UPR) that slows protein accumulation in the ER lumen and upregulates gene transcription of ER-resident chaperones and enzymes to relieve the ER stress. [12, 13] UPR activation is generally considered to be neuroprotective. [14, 15] However, in some adult white matter diseases, such as multiple sclerosis and Charcot-Marie-Tooth, [16] the UPR becomes maladaptive and induces apoptosis in myelinating glia. [17]

Information is scant on the UPR's role in ischemic brain injury. ER stress from ischemia and reperfusion activates the UPR, and it remains activated for 3 hours after HI in neonatal rats. [12] ER stress with UPR dysfunction also has been reported in adult rodent models of cerebral ischemia. [18] Whether the UPR persists for a longer duration after HI and during hypothermia and rewarming must be determined if we are to clarify the UPR's potential as a clinical biomarker or therapeutic target. Therefore, we used a piglet model of HI to test the hypotheses that 1) HI with normothermic recovery will activate the UPR whereas overnight hypothermia will suppress the UPR after HI; 2) rewarming will activate the UPR; and 3) UPR activation will be associated with apoptosis. We tested these hypotheses in white matter macroglial cells and cortical neurons and used the same rewarming rate of 0.5°C/hour that is used in clinical practice. [3]

MATERIALS AND METHODS

Animal preparation

All procedures were approved by the Johns Hopkins University Animal Care and Use Committee, and all protocols abided by the United States Public Health Service Policy on the Humane Care and Use of Laboratory Animals and the Guide for the Care and Use of Laboratory Animals. Animal care was in compliance with the National Institutes of Health Guidelines and ensured comfort throughout the experiments. Male piglets (3–5 days old, 1–2.5 kg) were randomized to receive HI injury or sham surgery. Piglets in the sham group received the same anesthetic, duration of anesthesia, and surgery as those in the HI group. The median age in each experimental group was 3–4 days. An age-matched, male, naïve group of piglets that did not receive anesthesia, surgery, or HI was an additional control group.

We anesthetized and intubated the piglets with oxygen, nitrous oxide, and isoflurane as previously described. [4] After inserting femoral arterial and venous catheters, which takes approximately 10–15 minutes, we discontinued the isoflurane, administered 70% nitrous oxide with 30% oxygen, and gave an intravenous (IV) bolus of fentanyl 20 μg/kg followed by a continuous infusion of 10–20 μg/kg/h. We administered vecuronium at 0.2 mg/kg/h IV to all piglets to prevent shivering during hypothermia and to ensure that all treatment groups received the same anesthetic regimen. We previously showed that this protocol does not alter the level of apoptosis above normal, baseline, developmental programmed cell death. [4, 5] Low-dose phenylephrine or dopamine infusions were initiated, when necessary, to maintain the piglets' mean arterial blood pressure at ≥45 mmHg and above the lower limit of autoregulation. [19] The piglets also received 5% dextrose in 0.45% saline at 10 ml/hour IV.

HI injury

We have previously reported the HI injury protocol. [4, 5, 19-21] Briefly, the inspired oxygen concentration is reduced to 10% for 45 minutes. A brief reoxygenation period with 21% oxygen for 5 minutes is used to increase the likelihood of cardiac resuscitation. Then, we clamp the endotracheal tube to produce 7–8 minutes of asphyxia. Piglets are resuscitated with chest compressions, 100 μg/kg epinephrine, and 50% oxygen. Piglets without return of spontaneous circulation (ROSC) after 3 minutes of compressions are excluded. Once ROSC is attained, we reduce the oxygen concentration to 30% for the rest of the experiment. The resultant metabolic acidosis is corrected with sodium bicarbonate, and hypocalcemia is treated with calcium chloride. Piglets evaluated by histology received 7 minutes of asphyxia, and piglets evaluated by immunoblotting received 7–8 minutes of asphyxia (11 pigs with 7 minutes of asphyxia and 7 pigs with 8 minutes of asphyxia).

Temperature

Piglets in the HI or sham groups were randomized to one of three temperature treatments as previously described [4, 5]: 1) normothermia (38.5–39.5°C), 2) whole body hypothermia (34.0°C), or 3) hypothermia followed by rewarming (0.5°C/hour) until the goal sample size in each group was reached. (Fig 1) This rewarming rate is the same as that used clinically. [3] In piglets assigned to receive hypothermia, we initiated cooling with ice packs and a

cooling blanket at 2 hours after ROSC (or the time equivalent in shams) to mimic clinical delays in hypothermia induction. In the rewarming groups, whole body temperature was increased beginning at 20 hours (after 18 h of hypothermia) at a goal rate of 0.5°C/hour until normothermia (38.5°C) was reached. All piglets were euthanized at 29 hours.

Histology

Pentobarbital (50 mg/kg, IV) was administered to achieve a deep level of anesthesia, and then piglets were transcardially perfused with cold phosphate-buffered saline (PBS) and 4% paraformaldehyde for brain tissue fixation. Paraffin embedded forebrains were cut into 10-μm sections. Anterior-posterior levels in coronal sections were matched according to anatomic regions.

We used immunoperoxidase histochemistry on paraffin sections as previously described [5] to identify neurons and macroglia that were positive for endoplasmic reticulum to nucleus signaling 1 (ERN1) in the cerebral cortex and subcortical white matter of the motor gyrus at the anterior striatal and posterior hippocampal levels. ERN1 is a marker of UPR activation also known as inositol requiring enzyme-1-α. [22] Mouse monoclonal IgG anti-ERN1 (1:200, Abgent, San Diego, CA) was used. We tested several ERN1 antibodies in piglet tissue for comparison to a positive control recombinant ERN1 protein (Origene, Rockville, MD). We chose the ERN1 antibody that had selective specificity in piglet tissue at the molecular weight that corresponded to the recombinant ERN1 protein; this antibody has been well characterized and used for immunocytochemistry. [23] In addition, we verified that our ERN1 antibody did not cross-react with a recombinant ERN2 protein (ABM, Inc., Richmond, BC, Canada) by western blot. To distinguish the morphology of microglial cells from that of oligodendrocytes and astrocytes, additional brain sections were incubated with the primary antibody anti-ionized calcium-binding adapter molecule 1 (Iba-1; 1:10, Wako, Richmond, VA). We developed the sections using 3,3′-diaminobenzidine substrate followed by a cresyl violet counterstain. Negative control tissue sections were exposed to secondary antibody without primary antibody.

A single investigator (JKL) who was blinded to treatment group manually counted ERN1+ and ERN1-negative macroglia in six random microscope fields in the center of the subcortical white matter of the motor gyrus at 1000X magnification with oil immersion. A second investigator (BW) who was also blinded to treatment group manually counted ERN1+ and ERN1-negative neurons on one side of the motor gyrus, from the sulcus between the cingulate and motor gyri to the tip of the motor gyrus, in cortical layers 2 and 3 and the beginning of layer 4 at 400X magnification. (Fig 2) Macroglia were identified by size (usually <10 μm in diameter) and distinguished from neurons by both size and neuronal morphologic criteria as previously reported. [5] Criteria for neuron identification included a large cell body (typically 8–20 μm in diameter), multipolar or triangular morphology, open non-condensed nucleus with chromatin strands and often a nucleolus. ERN1+ macroglia profiles were defined by intracellular brown staining within the nucleus and cytoplasm. ERN1+ neurons were identified by brown immunoreactivity seen as discrete foci within the nucleus. (Fig 3A–C). Microglia were distinguished from astrocytes and oligodendrocytes morphologically and immunophenotypically; microglia were not included in the ERN1 cell

counts. Microglia, as shown by Iba-1 immunoreactivity, have irregular and elongated nuclear morphology and soma with branch points and processes (Fig 3D). [24] We did not encounter activated, large, transformed microglia with a macrophage-like morphology in cortex or white matter. Therefore, putative astrocytes and oligodendrocytes were counted, but cells with a microglial morphology were not counted. An experimental neuropathologist (LJM) verified the identification and ERN1 classification of the macroglia and neurons.

To phenotype the ERN1+ macroglia in the white matter, we used immunofluorescence to co-label cells with ERN1, glial fibrillary acidic protein (GFAP), and 4',6-diamidino-2-phenylindole (DAPI) or with ERN1, oligodendrocyte transcription factor lineage protein-2 (olig2), and DAPI to identify astrocytes and oligodendrocytes, respectively, with intranuclear ERN1 staining. We used mouse monoclonal IgG anti-ERN1 primary antibody (1:50; Abgent) and rabbit polyclonal IgG anti-GFAP primary antibody (1:200, Dako, Carpinteria, CA) to immunophenotype ERN1+ astrocytes or mouse monoclonal IgG anti-ERN1 primary antibody (1:25; Abgent) and rabbit polyclonal IgG anti-olig2 primary antibody (1:20, GeneTex, Inc., Irvine, CA) to immunophenotype ERN1+ oligodendrocytes. We used the secondary antibodies goat polyclonal IgG anti-mouse Alexa Fluor 488 conjugate (1:50, Thermo Scientific, Rockford, IL) and goat polyclonal IgG anti-rabbit Alexa Fluor 555 conjugate (1:50, Thermo Scientific, Rockford, IL) as well as VectaShield hard set mounting medium with DAPI (Vector Laboratories, Burlingame, CA). Negative control tissue sections were incubated with fluorescent secondary antibody without primary antibody. We identified ERN1+ astrocytes by co-localization of GFAP (red) and intranuclear ERN1 (green; Fig 4A–D) under 1000X magnification with oil immersion using SPOT software (v5.1, Sterling Heights, MI). ERN1+ oligodendrocytes were identified by co-localization of olig2 (red) and intranuclear ERN1 (green; Fig 4E–H).

We used brightfield microscopy with immunoperoxidase to count ERN1+ cells (rather than immunofluorescence) to discern the cellular morphology and count oligodendrocytes and astrocytes with an oil objective lens at 1000X for optimal resolution when visualizing the fine granules of immunoreactivity in the nucleus. The observer needed to fine focus in the Z-axis focal plane to fully appreciate the ERN1 immunoreactivity. Standard epifluorescence microscopy of immunofluorescence in brain sections under oil immersion at 1000X has lower resolution.

We also evaluated the relationship between ERN1 immunoreactivity and apoptosis in the subcortical white matter. We previously reported white matter apoptotic profile counts using hematoxylin & eosin (H&E) stain and verified with terminal deoxynucleotidyl transferase dUTP nick end labeling in the piglets of the current study. The apoptosis occurred primarily among macroglia, including oligodendrocytes. [5] Apoptotic profiles were identified as cells with a few (<4) crescent-shaped or spherical clumps of chromatin, cytoplasmic condensation, cell shrinkage, eosinophilic cytoplasm, and an intact cytoplasmic membrane. [25] We used the H&E apoptotic profile counts from our prior study [5] to conduct paired comparisons of ERN1 immunoreactivity and apoptosis within pigs. Because apoptotic profiles are best visualized using our morphologic criteria by H&E stain [4, 5] and we evaluated ERN1 using immunohistochemistry with 3,3′-diaminobenzidine substrate, we could not directly correlate apoptotic profiles counts to ERN1+ macroglia counts in the same

microscope fields. Apoptotic profiles were instead compared to ERN1+ cell counts in the same region of interest – the subcortical white matter of the motor gyrus – at the striatal and hippocampal anatomic levels.

Immunoblotting

We examined ERN1, protein kinase RNA-like endoplasmic reticulum kinase (PERK), and heat shock protein 70 (HSP70) levels by immunoblotting. We cut fresh piglet brains into 1-cm slabs and obtained white matter punch samples with a dermal micropunch. Briefly, frozen lysates from the subcortical white matter of the sensorimotor cortex were homogenized in RIPA lysis buffer (Cell Signaling Technology, Danvers, MA) plus phosphatase inhibitor (Roche Applied Science, Penzberg, Germany), protease inhibitor cocktail (Invitrogen, Grand Island, NY), and reducing agent (DTT 50 mM, Sigma Aldrich) with a weight-to-volume ratio of 0.05 g to 300 μL. We determined the supernatant protein concentration using the Pierce BCA protein assay kit (Thermo Scientific, Carlsbad, CA). Protein samples (40 μg) were treated with loading buffer 4X (LDS sample buffer, Invitrogen), separated by sodium dodecyl sulfate-polyacrylamide gel electrophoresis, and used for western blotting as described. [4, 5] Blots were probed with monoclonal mouse anti-ERN1 IgG (1:500, Abgent), monoclonal rabbit anti-PERK IgG (1:1000, Cell Signaling Technology), and monoclonal mouse anti-HSP70 IgG (1:1000, Abcam, Cambridge MA). Immunoreactivity was detected by enhanced chemiluminescence (Thermo Scientific, Carlsbad, CA) to quantify the optical density. Band intensities were quantified using ImageLab v. 5.0 software (Bio-Rad Laboratories) with the Coomassie Brilliant Blue stain (Bio-Rad Laboratories, Philadelphia, PA) serving as the protein loading control. We normalized the ERN1, HSP70, and PERK optical densities to that of the Coomassie Brilliant Blue stain for analysis. In some experiments, we loaded positive controls with recombinant ERN1 protein (OriGene, Rockville, MD) and 293T cell lysate (ProSci, Poway, CA; positive controls for PERK and HSP70 antibodies). We ran brain homogenate from one piglet per group (naïve, sham+normothermia, sham+hypothermia, sham+rewarming, HI +normothermia, HI+hypothermia, and HI+ rewarming) on a single gel in four separate experiments.

Sample size calculations

Because we did not have *a priori* knowledge about the magnitude of change and variability in ERN1+ cell ratios that would be induced by hypothermia and rewarming after HI, we conducted a sample size estimate after four experiments had been completed in each of the HI+hypothermia and HI+rewarming groups. Preliminary data of ERN1+ macroglial ratios indicated a difference in means of 2.4% between the groups with a within-group standard deviation of 1.1%. To reject the null hypothesis that the ratio of ERN1+ macroglia would differ by less than 2.4% between HI piglets that receive sustained hypothermia and those that receive hypothermia with rewarming at a power of 0.8 with an alpha level of 0.05, we calculated that we would need 4 piglets/group. We chose sample sizes of 6–8 piglets/group to permit some error in our initial estimates of variability.

Statistical analysis

The mean total macroglial cell count was calculated from the sums of ERN1+ and ERN1-negative macroglia in 6 random microscope fields. The mean ratio of ERN1+ macroglia/total macroglia from 6 microscope fields was used for analysis. Neurons were analyzed as the total neuronal count (sum of ERN1+ and ERN1-negative neurons) and the ratio of ERN1+ neurons/total neurons. Significance was assumed at $p<0.05$.

To examine the effects of the anesthetic on the UPR, we used t-tests for parametric data and Mann Whitney rank sum tests for non-parametric data to compare the ratios of ERN1+ macroglia and neurons between naïve unanesthetized and normothermic sham piglets. To examine the effects of HI and temperature on the ERN1+ cell ratios and cell counts, we transformed non-parametric data with a log(x+1) function to generate parametric data when necessary. Then, a 2-way ANOVA was conducted with HI condition as factor 1 (sham or HI) and temperature as factor 2 (normothermia, hypothermia, or rewarming). We conducted *post-hoc* pairwise comparisons using the Holm Sidak method to examine the effects of HI injury when data were stratified by temperature and also to evaluate the effects of temperature when data were stratified by HI condition. We previously reported that hypothermia and rewarming promote macroglial apoptosis in the subcortical white matter of the motor gyrus in sham and HI piglets.[5] To evaluate the relationship between the UPR and apoptosis, we used Spearman correlations to conduct pairwise comparisons within pigs that had both ERN1+ ratios and apoptotic profile counts in macroglia [5] in the subcortical white matter of the motor gyrus. To analyze the immunoblot data, the densities of ERN1/Coomassie, PERK/Coomassie, and HSP70/Coomassie were normalized to naïve/Coomassie and then compared by Friedman two-way analysis of ranks with the four independent gels blocked as a between-subject factor.

Finally, we generated a summary table (table 3) using results from the current study and our previously published work in white matter apoptosis [5]. We conducted a 2-way ANOVA with HI condition as factor 1 (sham or HI) and temperature as factor 2 (normothermia, hypothermia, or rewarming). We then used *post-hoc* pairwise comparisons using the Holm Sidak method to compare the ERN1+ macroglia ratios, apoptotic profile counts from our prior study [5], and total macroglial cell counts in the subcortical white matter of the motor gyrus with normothermia as the control. Hypothermic or rewarmed sham piglets were compared to normothermic shams, and hypothermic or rewarmed HI piglets were compared to the normothermic HI piglets.

RESULTS

Mortality

Forty-four piglets underwent HI injury. One HI+normothermia piglet could not be resuscitated after asphyxia, and three HI+hypothermia piglets died from hypotension during anesthesia. Thus, 91% of the HI piglets completed the protocol with 29 hours of recovery under anesthesia. Forty-three piglets had sham surgery. One sham+normothermia and two sham+rewarming piglets died from hypotension during anesthesia. Thirteen naïve piglets that did not receive anesthesia or surgery were prepared as additional controls. In total, 93

piglets including those from our prior two studies [4, 5] were used in the final analysis. (Fig 1)

Physiology

We previously reported physiologic and blood gas data in the piglets, including temperature, blood pressure, oxyhemoglobin saturation, pH, $PaCO_2$, hemoglobin, and electrolyte levels, in our previous reports on cortical neuron [4] and white matter apoptosis. [5] In addition, mean glucose levels were 186 mg/dL (SD: 95) in rewarmed and 148 mg/dL (SD: 71) in hypothermic shams. We summarize select parameters during the HI protocol here to describe the physiologic severity of the HI injury. During hypoxia, the mean oxyhemoglobin saturations were 25% (SD: 7) in HI+normothermia (n=6), 30% (SD: 9) in HI+hypothermia (n=8), and 29% (SD: 7) in HI+rewarming (n=8) groups. The oxyhemoglobin saturations decreased during asphyxia to 7% (SD: 11) in HI+normothermia, 7% (SD: 3) in HI +hypothermia, and 4% (SD: 3) in HI+rewarming piglets. Hypothermic piglets had core temperatures of approximately 34°C and were successfully rewarmed to normothermia without exceeding the goal temperature.

Anesthetic minimally affects the UPR

We first evaluated the effect of the anesthetic on the UPR. The ratios of ERN1+ macroglia and ERN1+ neurons were similar between naïve unanesthetized piglets and anesthetized normothermic sham piglets at the striatal (p=0.694 for macroglia; p=0.867 for neurons) and hippocampal levels (p=0.452 for macroglia; p=0.950 for neurons; Fig 5). Therefore, the anesthetic regimen and surgical preparation had minimal effect on the UPR.

The macroglial UPR is affected by HI, hypothermia, and rewarming and is associated with apoptosis

HI (p<0.001) and temperature (p=0.046) independently and interactively (p<0.001) affected the ERN1+ macroglia ratio at the striatal level. The ERN1+ cells in the subcortical white matter were immunophenotyped as oligodendrocytes and astrocytes (Fig 4). When data were stratified by HI injury, normothermic (p=0.015) and rewarmed (p=0.014) HI piglets had greater ERN1+ macroglia ratios than did HI piglets that remained hypothermic (Fig 6A). Among shams, sustained hypothermia (p=0.011) and rewarming (p=0.004) each increased the macroglial ERN1+ ratio above that in normothermia. When data were stratified by temperature, hypothermic shams had greater ERN1+ macroglial ratios than did hypothermic HI piglets (p<0.001). Rewarmed shams also had more ERN1+ macroglia than did rewarmed HI piglets (p=0.004). Absolute cell counts and ERN1+ cell ratios are presented in Tables 1 and 2.

HI (p=0.002), but not temperature (p=0.349), affected the total macroglial cell counts (ERN1+ plus ERN1-negative) with an interactive effect (p<0.001) in white matter at the striatal level (Fig 6B). When data were stratified by injury, HI piglets that remained normothermic had fewer macroglial cells than did HI piglets that were rewarmed (p=0.018). Normothermic shams had more macroglia than did hypothermic (p=0.009) and rewarmed (p=0.007) shams. Among the hypothermic groups, HI piglets had more macroglia than did

shams (p=0.011). Similarly, HI rewarmed piglets had more macroglia than sham rewarmed piglets (p<0.001).

At the posterior hippocampal anatomic level, only temperature affected the ERN1+ macroglia ratio (p=0.009); HI did not have an effect (p=0.244, Fig 6C). When we controlled for HI, rewarming increased the ERN1+ macroglia ratio more than normothermia (p=0.007). In comparisons stratified by injury, rewarmed shams had more ERN1+ macroglia than did normothermic shams (p=0.024). One rewarmed sham piglet did not have ERN1 macroglia counts because the subcortical white matter had tissue damage artifact at the hippocampal anatomic level. (The cortical tissue was not damaged and neurons were counted in this piglet.) The number of macroglia in white matter was not affected by HI (p=0.516) or temperature (p=0.392; Fig 6D) at the hippocampal level.

We previously reported that hypothermia and rewarming promote apoptosis in the subcortical white matter of the motor gyrus and other white matter regions in sham and HI piglets. [5] Among piglets that had both ERN1+ macroglia and apoptotic profile counts at the striatal level, [5] the ratio of ERN1+ macroglia correlated to the number of apoptotic profiles in the motor subcortical white matter in shams that received normothermia, hypothermia, or rewarming (p=0.026; Fig 7A). ERN1+ and apoptotic macroglial counts were not correlated in HI piglets after normothermia, hypothermia, or rewarming (p=0.956; Fig 7B). At the hippocampal level, the ratio of ERN1+ macroglia did not correlate with the number of apoptotic profiles in the subcortical white matter of sham (n=21; r=0.109; p=0.633) or HI piglets (n=22; r=0.269; p=0.222).

HI, hypothermia, and rewarming decrease neuron counts without affecting the neuronal UPR

Absolute cell counts and ratios for ERN1+ neurons are presented in Tables 1 and 2. Neither HI (p=0.104) nor temperature (p=0.738) affected the ratio of ERN1+ neurons in the motor cortex at the striatal level (Fig 8A). Both HI (p=0.019) and temperature (p=0.002) affected the number of neurons without an interaction (p=0.120; Fig 8B). When we controlled for HI, rewarming decreased the number of neurons relative to normothermia (p=0.001). *Post-hoc* comparisons showed that rewarmed shams had fewer neurons than did normothermic (p<0.001) and hypothermic (p=0.045) shams. Moreover, rewarmed shams had lower neuronal cell counts than did rewarmed HI piglets (p=0.003).

At the hippocampal level, HI (p=0.251) and temperature (p=0.070) did not influence the ratio of ERN1+ neurons in the motor cortex (Fig 8C). Temperature (p=0.005), but not HI (p=0.798), affected the neuronal count (Fig 8D) without an interaction (p=0.703). When we controlled for HI, both hypothermia (p=0.006) and rewarming (p=0.022) decreased the number of neurons below that observed during normothermia. In *post-hoc* comparisons, normothermic HI piglets had more neurons than did hypothermic HI piglets (p=0.043). Neuron counts could not be completed in one HI+normothermia and three HI+rewarming piglets because of cortical damage to the mounted tissue; the entire motor cortex must be intact to quantify ERN1+ and ERN1-negative neurons. (These pigs had intact subcortical white matter, however, and thus had macroglial cell counts.)

Immunoblotting showed similar levels of ERN1, PERK, and HSP70 levels among groups

Immunoreactivity on Western blots for ERN1 (p=0.345), PERK (p=0.297), and HSP70 (p=0.836) was similar among normothermic sham, hypothermic sham, rewarmed sham, normothermic HI, hypothermic HI, and rewarmed HI piglets (Fig 9).

DISCUSSION

This study identifies potential deleterious, cell type-specific effects from delayed hypothermia and rewarming on the newborn brain. We determined in a neonatal piglet model that hypothermia and rewarming cause macroglial ER stress that is associated with white matter apoptosis independent of HI. These findings have critical and clinically relevant implications for the use of hypothermia in the developing brain. First, temperature and HI affected the UPR in oligodendrocytes and astrocytes both independently and interactively. Both sustained hypothermia and hypothermia with rewarming increased the ERN1+ macroglia ratio above that of normothermia in shams, whereas HI prior to hypothermia diminished the macroglial UPR. Second, macroglial UPR activation correlated with white matter apoptosis as measured in our prior study [5] in shams, thereby associating UPR activation with white matter apoptosis after hypothermia and rewarming. This apoptosis was robust and decreased oligodendrocyte and astrocyte cell counts in shams. However, the associations between macroglial UPR activation and apoptosis with hypothermia and rewarming were not observed after HI. Third, hypothermia and rewarming induced cortical neuron loss in the motor gyrus, but this change was not related to ERN1 upregulation. Pre-hypothermia HI blocked the macroglial cell loss after hypothermia and rewarming but did not influence the cortical neuron sensitivity to hypothermia and rewarming. Altogether, these findings lead us to conclude that in the neonatal brain: 1) hypothermia and rewarming activate the UPR in oligodendrocytes and astrocytes and promote white matter apoptosis independent of HI; 2) hypothermia and rewarming induce cortical neuron loss through mechanisms not clearly associated with the UPR; and 3) HI may interrupt the macroglial ER stress response and subsequent cell death with promotion of apoptosis by mechanisms separate from the hypothermia-induced UPR. (Table 3) The potential cytotoxic effects of hypothermia and rewarming on oligodendrocytes, astrocytes, and neurons in uninjured or minimally injured developing brain deserve further study given increasing interest in treating mild HIE with hypothermia and for designing clinical studies. [26]

Therapeutic hypothermia initiated during the latent phase soon after HI [27] is neuroprotective in part by attenuating secondary energy failure. [28] Disturbed cerebral metabolism with mitochondrial dysfunction occurs early after HI [29] with secondary energy failure at approximately 24 hours in a piglet HI model of hypoxia with carotid occlusion; hypothermia for 12 hours mitigates the energy failure through 60 hours. [30] In our piglet HI model of whole-body hypoxia-asphyxia, mitochdondrial failure occurs by 12 hours with normothermia. [31] We therefore expect that the 18-29 hours of hypothermia in our protocols targeted the latent phase after HI prior to secondary deterioration. [27] We did not extend hypothermia to 72 hours, the duration used in the clinical treatment of HIE, due to neurotoxic effects of the anesthetic (unpublished data) and limited resources. Hypothermia confers neuroprotection in our piglet HI model by preserving viable neurons

and reducing NMDA receptor activation, nitric oxide synthase relocalization, oxidative stress, and cellular necrosis. [32-35] However, hypothermia may promote apoptosis in cortex after HI [4] and in white matter with or without HI [5], which may reflect an off-target effect of hypothermia and rewarming.

Based on the similar ERN1+ macroglia and neuron ratios between sham normothermic and naïve unanesthetized piglets, our 29 hour anesthetic minimally affected the UPR in brain. We hypothesized that HI would induce ER stress with UPR activation, that post-HI hypothermia would suppress the UPR, and that cellular stress from rewarming would reactivate the UPR. We formulated these hypotheses based on our prior observations in HI piglets [31] and assumptions that hypothermia would decrease protein translation and rewarming would reinitiate translation. [36] Morphological and biochemical evidence for ER stress has been identified in piglet striatum using a variation of the model used here. [31] Electron microscopy has shown ER damage with 3-6 h after HI and prominent release of ER luminal protein by 3 h after HI. [31] Biochemical and morphological evidence for ER stress in brain has been found in neonatal rodent HI models with 3 hours of recovery. [12] ER stress from HI activates the protein kinase activity of PERK, an ER-resident protein that phosphorylates the eukaryotic initiation factor-2 α-subunit (eIF2-α), to slow translation of mRNA to protein [12, 37] and activate the UPR. [38] Ischemia also impairs heat shock protein translation in immature brain [39]: heat shock proteins facilitate *de novo* protein folding and refolding of misfolded proteins. Impaired heat shock protein function after HI would cause protein misfolding and compound the ER stress.

These perturbations could influence neural cell viability. A recent study of HI in neonatal mice found an association between ER stress and a newly described form of cortical neuron degeneration called macrozeiosis. [40] This neurodegeneration was morphologically distinct from necrosis and classical apoptosis and had a characteristic signature typified by cytoplasmic shedding. [40] In our piglet study, hypothermia and rewarming induced cortical neuron loss. While the mechanism for this neuronal elimination is not known, it was distinct from the ER stress-associated induction of apoptosis in white matter macroglia. This study starkly emphasizes the need for histological verification of the cell types in which the UPR is occurring.

We designed our study to examine the independent effects of temperature and HI and the interaction between the two factors. Our experimental design included normothermia with or without prior HI; sustained hypothermia with or without prior HI; and hypothermia followed by rewarming with or without prior HI. Each group provided relevant information about the UPR and cell death.

Piglets that remained hypothermic after HI had lower ERN1+ macroglia ratios than did HI normothermic piglets. Our histologic measurements focused on oligodendrocytes and astrocytes. This finding suggests that post-HI hypothermia suppressed the UPR through 29 hours of recovery. The ability of hypothermia to mitigate ER stress in piglet brain and presumably protein misfolding after HI may be related to decreased cell metabolism, protein translation, [41] and oxidative stress [42] and modulation of the inflammatory response. [43]

HI piglets treated with hypothermia have diminished NMDA receptor activation, nitric oxide synthase activation, and oxidized protein burden. [32]

In contrast to our observations after HI, hypothermia increased the ERN1+ macroglia ratio above that of normothermia in sham piglets. Thus, hypothermia itself appears to induce ER stress with UPR activation in oligodendrocytes and astrocytes, and prior HI may interrupt the hypothermia-induced ER stress. It was previously shown that hypoxic preconditioning decreases caspase-12 activation in hippocampal slice cultures exposed to oxygen-glucose deprivation [44] and that caspase-12 is linked to neuronal cell death in rodents with ER stress after ischemia. [13] However, the role of capsase-12 in human neurodegeneration is uncertain because this gene has acquired polymorphisms during evolution that cause it to encode for a truncated protein without caspase activity. [45]

Rewarming also promoted macroglial UPR activation. Rewarmed HI piglets had higher ERN1+ macroglia ratios than did HI piglets that remained hypothermic, and rewarming activated the UPR above that observed during normothermia in shams. Therefore, the ER stress response could provide a potential target for adjuvant therapies to reduce the risk of neurologic injury from rewarming in HIE. [46-48] Because all piglets were studied at 29 hours of recovery after HI or sham surgery, the rewarmed groups received shorter duration of hypothermia than those that remained hypothermic. The observed UPR activation in rewarmed HI piglets could also reflect shorter duration of hypothermia. Nonetheless, other studies corroborate the potential cytotoxic effects of rewarming. For example, faster rewarming rates from hypothermic cardiopulmonary bypass are also associated with stroke and higher plasma glial fibrillary acidic protein levels, a marker of astrocyte injury. [49] Rewarming reinitiates protein translation through dephosphorylation of eIF2-α in mammalian cells recovering from cold shock. [36] Upregulated protein translation with the accumulation of misfolded proteins in addition to cellular stressors from hypothermia with rewarming, such as inflammation [50] and oxidative stress, [35, 51, 52] may activate the UPR. [53, 54]

Furthermore, the ratio of ERN1+ macroglia correlated with apoptosis in the subcortical white matter of sham piglets. [5] Congruent with our findings that hypothermia and rewarming activate the UPR, both sustained hypothermia and hypothermia with rewarming reduced the macroglial cell count below that of normothermia in shams. The increasing interest in therapeutic hypothermia for mild HIE and the routine use of hypothermic cardiopulmonary bypass for neonatal and pediatric cardiac surgery warrants investigation into the off-targets effects of hypothermia and rewarming. Hypothermia and rewarming may have deleterious effects in the uninjured or minimally injured developing white matter, including the UPR activation, apoptosis, and oligodendrocyte and astrocyte loss observed in our sham piglets.

HI prior to hypothermia prevented macroglial cell loss from sustained hypothermia and hypothermia with rewarming. Perhaps HI enabled macroglia to tolerate the proteomic stress of hypothermia, or HI interrupted or impaired the mechanisms required to fully execute the UPR with apoptosis. For example in HI piglet striatum, the ER shows evidence for pathological damage by 3 h [31] so the UPR might not be operative. Hypothermia and

rewarming without HI, however, resulted in a robust UPR with apoptosis in white matter macroglia.

The relationships between HI, hypothermia, rewarming, and ERN-related UPR were limited to oligodendrocytes and astrocytes. The ratio of ERN1+ neurons was not associated with HI or temperature at 29 hours of recovery, thereby demonstrating differential activation of the UPR among specific cell types and anatomic regions. The UPR's importance in neurologic injury after HI may be focused on white matter injury and might serve as a target for adjuvant therapies designed to decrease white matter injury in HIE. White matter injury remains a prominent component of neurologic injury in HIE despite the use of therapeutic hypothermia, [46, 47] and white matter injuries predict neurodevelopmental outcomes in survivors of HIE. [7] The difference in cell-specific UPR activation may be due to high protein synthesis in myelinating glia [55] that could impart vulnerability to temperature-related ER stress. The UPR is associated with apoptosis in myelinating glia in multiple sclerosis and Charcot-Marie-Tooth. [16, 17] Astrocytes are also highly metabolically active cells that are activated by hypothermia and oxygen-glucose deprivation. [56] They are involved in neurotransmitter and ion clearance from the interstitial space, [57, 58] neuroinflammation, [59] brain development, and cell differentiation, proliferation, and plasticity. [60] It is also possible that the neuronal UPR subsided by 29 hours of recovery.

Sustained hypothermia and hypothermia with rewarming decreased the number of neurons in the motor cortex below that of normothermia. The cytotoxic effects of hypothermia and rewarming in neurons were independent of HI and not related to robust ERN1-related UPR activation within neurons. This again highlights the potential deleterious effects of hypothermia and rewarming to the developing brain in the absence of moderate or severe HI and in uninjured brain regions remote from areas of moderate or severe injury. The risks of cooling neonates for mild HIE must be further studied. Hypothermia after HI also reduced the number of cortical neurons relative to that observed with normothermia after HI. We observed intracortical gyrus differences in the magnitude of cortical neuron loss and white matter changes at striatal and hippocampal levels, but these differences could be due to differences in cortical connectivity that can be found even within the same gyrus. [61] Additional experiments are necessary to identify the mechanisms responsible for this rapid cortical neuron loss.

Our Western blotting experiments did not show evidence for UPR activation in white matter extracts, but our histologic data revealed strong evidence for UPR activation. Western blotting may be limited by the use of a crude homogenate in which sources of protein include all glial cells, neurons, axons, and vascular and blood-borne cells. In contrast, histologic evaluation permits high resolution identification and precise counting of macroglia with intranuclear ERN1+ foci. It is also possible that the magnitudes of between-group differences in ERN1, PERK, and HSP70 protein expression were too small to be detected in a crude homogenate assay. We previously demonstrated increased levels of cortical cleaved caspase-3 after hypothermia and rewarming following HI in our model. [4]

Our study had some limitations. Although we conducted a power analysis to determine our sample sizes, the number of piglets per experimental group was small, and we used only

males. The animals remained under general anesthesia for 29 hours for comfort, a practice that is not used clinically. Nonetheless, the fact that the ratios of ERN1+ macroglia and neurons were similar between unanesthetized naïve and anesthetized sham normothermic piglets indicated that the anesthetic minimally affected the UPR. Another limitation is that we examined only one time point and only one histologic marker for UPR after HI or sham surgery; the neuronal UPR response may have subsided by 29 hours, and we cannot define a timeline for macroglial UPR activation during hypothermia and rewarming. Moreover, clinical hypothermia for HIE is provided for more than 24 hours. Therefore, the UPR needs to be examined during longer durations of hypothermia to define the UPR's potential as a clinical biomarker or target for adjuvant therapies. Extending hypothermia beyond 72 hours, however, may not be beneficial and could affect neuroinflammation [62] and exacerbate cortical neuron loss. Although we cannot determine whether white matter macroglial UPR activation will result in long-term neurologic consequences, in clinical MRI studies white matter injury is evident 2 weeks after therapeutic hypothermia,[46, 47] and is associated with neurodevelopmental impairments at 2 years of age.[63] The possible effect of HI in disengaging the UPR during hypothermia and rewarming is difficult to apply clinically, and different degrees of hypoxia may affect subsequent responses to cellular stresses differently. HI did not activate the UPR above that observed after sham surgery during 29 hours normothermic recovery. The UPR may have subsided at this relatively late time point as other studies demonstrate UPR activation in rodents 3 hours after HI. [12] Microglia may also be involved in the UPR, and we did not evaluate ERN1 upregulation in microglia. Glucose was not well controlled, and hyperglycemia can contribute to UPR activation. [64]

CONCLUSION

We identified that hypothermia and rewarming induce ER stress with UPR activation in oligodendrocytes and astrocytes of the developing brain. Our finding that macroglial UPR activation was associated with apoptosis and a decrease in macroglial cell count in shams demonstrated that hypothermia and rewarming are neurotoxic independent of HI. Hypothermia and rewarming also caused cortical neuron loss independent of HI and unassociated with UPR activation. Pre-hypothermia HI interrupts the UPR during hypothermia and rewarming. Modulating the UPR in macroglial cells and the maladaptive responses of cortical neurons during hypothermia and rewarming could improve neuroprotection in the white matter and cerebral cortex during clinical situations that warrant the therapeutic use of hypothermia.

Acknowledgements

Dr. Lee was supported by grants from the National Institutes of Health (NIH; K08 NS080984 [NINDS]; R21HD072845 [NICHD]), a Johns Hopkins University Clinician Scientist Award, and an American Heart Association Grant-in-Aid. Drs. Koehler and Martin were supported by a grant from the NIH (R01 NS060703). Dr. Martin was also supported by a grant from NIH NINDS (R01 NS079348). Dr. Lee has research funding from Medtronic for a clinical study. We are grateful to Claire Levine, MS, ELS, for her editorial assistance and to Dawn Spicer for her assistance with the immunohistochemistry.

Abbreviations

DAPI 4',6-diamidino-2-phenylindole

ER	endoplasmic reticulum
ERN1	endoplasmic reticulum to nucleus signaling-1 protein
GFAP	macroglial fibrillary acidic protein
HSP70	heat shock protein 70
HI	hypoxia-ischemia
Iba-1	ionized calcium-binding adaptor molecule 1
IQR	interquartile range
Olig2	oligodendrocyte transcription factor lineage protein-2
PERK	protein kinase RNA-like endoplasmic reticulum kinase
SD	standard deviation
UPR	unfolded protein response

References

1. Azzopardi D, Strohm B, Marlow N, et al. Effects of hypothermia for perinatal asphyxia on childhood outcomes. N Engl J Med. 2014; 371:140–149. [PubMed: 25006720]
2. Shankaran S, Pappas A, McDonald SA, et al. Childhood outcomes after hypothermia for neonatal encephalopathy. N Engl J Med. 2012; 366:2085–2092. [PubMed: 22646631]
3. Shankaran S, Laptook AR, Ehrenkranz RA, et al. Whole-body hypothermia for neonates with hypoxic-ischemic encephalopathy. N Engl J Med. 2005; 353:1574–1584. [PubMed: 16221780]
4. Wang B, Armstrong JS, Lee JH, et al. Rewarming from therapeutic hypothermia induces cortical neuron apoptosis in a swine model of neonatal hypoxic-ischemic encephalopathy. J Cereb Blood Flow Metab. 2015
5. Wang B, Armstrong JS, Reyes M, et al. White matter apoptosis is increased by delayed hypothermia and rewarming in a neonatal piglet model of hypoxic ischemic encephalopathy. Neuroscience. 2016 In press.
6. van Schie PE, Schijns J, Becher JG, Barkhof F, van Weissenbruch MM, Vermeulen RJ. Long-term motor and behavioral outcome after perinatal hypoxic-ischemic encephalopathy. Eur J Paediatr Neurol. 2015; 19:354–359. [PubMed: 25683783]
7. Cavalleri F, Lugli L, Pugliese M, et al. Prognostic value of diffusion-weighted imaging summation scores or apparent diffusion coefficient maps in newborns with hypoxic-ischemic encephalopathy. Pediatr Radiol. 2014; 44:1141–1154. [PubMed: 24715056]
8. Sun H, Tang Y, Li L, Guan X, Wang D. Effects of local hypothermia on neuronal cell apoptosis after intracerebral hemorrhage in rats. J Nutr Health Aging. 2015; 19:291–298. [PubMed: 25732214]
9. Zhu X, Zelmer A, Kapfhammer JP, Wellmann S. Cold-inducible RBM3 inhibits PERK phosphorylation through cooperation with NF90 to protect cells from endoplasmic reticulum stress. FASEB J. 2015
10. Prieto Robles C, Argibay Lago A, Hernanz Del Rio A, Rodriguez Castano IM, Fernandez-Rodriguez D. Optimization of glucose metabolism in patients undergoing therapeutic hypothermia after sudden cardiac arrest. Rev Enferm. 2015; 38:46–50.
11. Yu A, Li P, Tang T, Wang J, Chen Y, Liu L. Roles of Hsp70s in stress responses of microorganisms, plants, and animals. Biomed Res Int. 2015; 2015:510319. [PubMed: 26649306]
12. Badiola N, Penas C, Minano-Molina A, et al. Induction of ER stress in response to oxygen-glucose deprivation of cortical cultures involves the activation of the PERK and IRE-1 pathways and of caspase-12. Cell Death Dis. 2011; 2:e149. [PubMed: 21525936]

13. Nakka VP, Gusain A, Raghubir R. Endoplasmic reticulum stress plays critical role in brain damage after cerebral ischemia/reperfusion in rats. Neurotox Res. 2010; 17:189–202. [PubMed: 19763736]
14. Smith HL, Li W, Cheetham ME. Molecular chaperones and neuronal proteostasis. Semin Cell Dev Biol. 2015; 40:142–152. [PubMed: 25770416]
15. Rzechorzek NM, Connick P, Patani R, Selvaraj BT, Chandran S. Hypothermic preconditioning of human cortical neurons requires proteostatic priming. EBioMedicine. 2015; 2:528–535. [PubMed: 26287272]
16. Lin W, Popko B. Endoplasmic reticulum stress in disorders of myelinating cells. Nat Neurosci. 2009; 12:379–385. [PubMed: 19287390]
17. Gow A, Wrabetz L. CHOP and the endoplasmic reticulum stress response in myelinating glia. Curr Opin Neurobiol. 2009; 19:505–510. [PubMed: 19744850]
18. Kumar R, Krause GS, Yoshida H, Mori K, DeGracia DJ. Dysfunction of the unfolded protein response during global brain ischemia and reperfusion. J Cereb Blood Flow Metab. 2003; 23:462–471. [PubMed: 12679723]
19. Larson AC, Jamrogowicz JL, Kulikowicz E, et al. Cerebrovascular autoregulation after rewarming from hypothermia in a neonatal swine model of asphyxic brain injury. J Appl Physiol (1985). 2013; 115:1433–1442. [PubMed: 24009008]
20. Lee JK, Brady KM, Mytar JO, et al. Cerebral blood flow and cerebrovascular autoregulation in a swine model of pediatric cardiac arrest and hypothermia. Crit Care Med. 2011; 39:2337–2345. [PubMed: 21705904]
21. Lee JK, Yang ZJ, Wang B, et al. Noninvasive autoregulation monitoring in a swine model of pediatric cardiac arrest. Anesth Analg. 2012; 114:825–836. [PubMed: 22314692]
22. Chonghaile TN, Gupta S, John M, Szegezdi E, Logue SE, Samali A. BCL-2 modulates the unfolded protein response by enhancing splicing of X-box binding protein-1. Biochem Biophys Res Commun. 2015; 466:40–45. [PubMed: 26319553]
23. Hyrskyluoto A, Bruelle C, Lundh SH, et al. Ubiquitin-specific protease-14 reduces cellular aggregates and protects against mutant huntingtin-induced cell degeneration: Involvement of the proteasome and ER stress-activated kinase IRE1alpha. Hum Mol Genet. 2014; 23:5928–5939. [PubMed: 24951540]
24. Lafrenaye AD, Todani M, Walker SA, Povlishock JT. Microglia processes associate with diffusely injured axons following mild traumatic brain injury in the micro pig. J Neuroinflammation. 2015; 12:186–015-0405-6. [PubMed: 26438203]
25. Martin LJ, Al-Abdulla NA, Brambrink AM, Kirsch JR, Sieber FE, Portera-Cailliau C. Neurodegeneration in excitotoxicity, global cerebral ischemia, and target deprivation: A perspective on the contributions of apoptosis and necrosis. Brain Res Bull. 1998; 46:281–309. [PubMed: 9671259]
26. Tagin M, Zhu C, Gunn AJ. Beneficence and nonmaleficence in treating neonatal hypoxicischemic brain injury. Dev Neurosci. 2015; 37:305–310. [PubMed: 25720376]
27. Gunn AJ, Gluckman PD. Head cooling for neonatal encephalopathy: The state of the art. Clin Obstet Gynecol. 2007; 50:636–651. [PubMed: 17762415]
28. Thornton C, Hagberg H. Role of mitochondria in apoptotic and necroptotic cell death in the developing brain. Clin Chim Acta. 2015; 451:35–38. [PubMed: 25661091]
29. Bainbridge A, Tachtsidis I, Faulkner SD, et al. Brain mitochondrial oxidative metabolism during and after cerebral hypoxia-ischemia studied by simultaneous phosphorus magnetic-resonance and broadband near-infrared spectroscopy. Neuroimage. 2014; 102(Pt 1):173–183. [PubMed: 23959202]
30. Thoresen M, Penrice J, Lorek A, et al. Mild hypothermia after severe transient hypoxiaischemia ameliorates delayed cerebral energy failure in the newborn piglet. Pediatr Res. 1995; 37:667–670. [PubMed: 7603788]
31. Martin LJ, Brambrink AM, Price AC, et al. Neuronal death in newborn striatum after hypoxiaischemia is necrosis and evolves with oxidative stress. Neurobiol Dis. 2000; 7:169–191. [PubMed: 10860783]

32. Mueller-Burke D, Koehler RC, Martin LJ. Rapid NMDA receptor phosphorylation and oxidative stress precede striatal neurodegeneration after hypoxic ischemia in newborn piglets and are attenuated with hypothermia. Int J Dev Neurosci. 2008; 26:67–76. [PubMed: 17950559]
33. Agnew DM, Koehler RC, Guerguerian AM, et al. Hypothermia for 24 hours after asphyxic cardiac arrest in piglets provides striatal neuroprotection that is sustained 10 days after rewarming. Pediatr Res. 2003; 54:253–262. [PubMed: 12736390]
34. Ni X, Yang ZJ, Wang B, et al. Early antioxidant treatment and delayed hypothermia after hypoxia-ischemia have no additive neuroprotection in newborn pigs. Anesth Analg. 2012; 115:627–637. [PubMed: 22745113]
35. Zhu J, Wang B, Lee JH, et al. Additive neuroprotection of a 20-HETE inhibitor with delayed therapeutic hypothermia after hypoxia-ischemia in neonatal piglets. Dev Neurosci. 2015; 37:376–389. [PubMed: 25721266]
36. Hofmann S, Cherkasova V, Bankhead P, Bukau B, Stoecklin G. Translation suppression promotes stress granule formation and cell survival in response to cold shock. Mol Biol Cell. 2012; 23:3786–3800. [PubMed: 22875991]
37. Harding HP, Zhang Y, Ron D. Protein translation and folding are coupled by an endoplasmicreticulum-resident kinase. Nature. 1999; 397:271–274. [PubMed: 9930704]
38. Lu M, Lawrence DA, Marsters S, et al. Opposing unfolded-protein-response signals converge on death receptor 5 to control apoptosis. Science. 2014; 345:98–101. [PubMed: 24994655]
39. Sun X, Crawford R, Liu C, Luo T, Hu B. Development-dependent regulation of molecular chaperones after hypoxia-ischemia. Neurobiol Dis. 2015; 82:123–131. [PubMed: 26070787]
40. Chavez-Valdez R, Flock DL, Martin LJ, Northington FJ. Endoplasmic reticulum pathology and stress response in neurons precede programmed necrosis after neonatal hypoxia-ischemia. Int J Dev Neurosci. 2016; 48:58–70. [PubMed: 26643212]
41. Knight JR, Bastide A, Roobol A, et al. Eukaryotic elongation factor 2 kinase regulates the cold stress response by slowing translation elongation. Biochem J. 2015; 465:227–238. [PubMed: 25353634]
42. Zhao H, Chen Y. Effects of mild hypothermia therapy on the levels of glutathione in rabbit blood and cerebrospinal fluid after cardiopulmonary resuscitation. Iran J Basic Med Sci. 2015; 18:194–198. [PubMed: 25810895]
43. Yuan X, Ghosh N, McFadden B, et al. Hypothermia modulates cytokine responses after neonatal rat hypoxic-ischemic injury and reduces brain damage. ASN Neuro. 2014; 6 10.1177/1759091414558418. Print 2014.
44. Bickler PE, Clark JP, Gabatto P, Brosnan H. Hypoxic preconditioning and cell death from oxygen/glucose deprivation co-opt a subset of the unfolded protein response in hippocampal neurons. Neuroscience. 2015; 310:306–321. [PubMed: 26404874]
45. Fischer H, Koenig U, Eckhart L, Tschachler E. Human caspase 12 has acquired deleterious mutations. Biochem Biophys Res Commun. 2002; 293:722–726. [PubMed: 12054529]
46. Tekes A, Poretti A, Scheurkogel MM, et al. Apparent diffusion coefficient scalars correlate with near-infrared spectroscopy markers of cerebrovascular autoregulation in neonates cooled for perinatal hypoxic-ischemic injury. AJNR Am J Neuroradiol. 2015; 36:188–193. [PubMed: 25169927]
47. Howlett JA, Northington FJ, Gilmore MM, et al. Cerebrovascular autoregulation and neurologic injury in neonatal hypoxic-ischemic encephalopathy. Pediatr Res. 2013; 74:525–535. [PubMed: 23942555]
48. Burton VJ, Gerner G, Cristofalo E, et al. A pilot cohort study of cerebral autoregulation and 2-year neurodevelopmental outcomes in neonates with hypoxic-ischemic encephalopathy who received therapeutic hypothermia. BMC Neurol. 2015; 15:209–015-0464-4. [PubMed: 26486728]
49. Hori D, Everett AD, Lee JK, et al. Rewarming rate during cardiopulmonary bypass is associated with release of glial fibrillary acidic protein. Ann Thorac Surg. 2015; 100:1353–1358. [PubMed: 26163357]
50. Bisschops LL, Hoedemaekers CW, Mollnes TE, van der Hoeven JG. Rewarming after hypothermia after cardiac arrest shifts the inflammatory balance. Crit Care Med. 2011

51. Dohi K, Miyamoto K, Fukuda K, et al. Status of systemic oxidative stress during therapeutic hypothermia in patients with post-cardiac arrest syndrome. Oxid Med Cell Longev. 2013; 2013:562429. [PubMed: 24066191]
52. Alva N, Palomeque J, Carbonell T. Oxidative stress and antioxidant activity in hypothermia and rewarming: Can RONS modulate the beneficial effects of therapeutic hypothermia? Oxid Med Cell Longev. 2013; 2013:957054. [PubMed: 24363826]
53. Guerra R, Vera-Aguilar E, Uribe-Ramirez M, et al. Exposure to inhaled particulate matter activates early markers of oxidative stress, inflammation and unfolded protein response in rat striatum. Toxicol Lett. 2013; 222:146–154. [PubMed: 23892126]
54. Llorente IL, Burgin TC, Perez-Rodriguez D, Martinez-Villayandre B, Perez-Garcia CC, Fernandez-Lopez A. Unfolded protein response to global ischemia following 48 h of reperfusion in the rat brain: The effect of age and meloxicam. J Neurochem. 2013; 127:701–710. [PubMed: 23763503]
55. Millson GC, Hunter GD. Protein synthesis in normal and scrapie mouse brain. J Neurochem. 1968; 15:447–453. [PubMed: 5691263]
56. Agematsu K, Korotcova L, Morton PD, Gallo V, Jonas RA, Ishibashi N. Hypoxia diminishes the protective function of white-matter astrocytes in the developing brain. J Thorac Cardiovasc Surg. 2016; 151:265–272. e3. [PubMed: 26412317]
57. Oberheim NA, Takano T, Han X, et al. Uniquely hominid features of adult human astrocytes. J Neurosci. 2009; 29:3276–3287. [PubMed: 19279265]
58. Araque A, Carmignoto G, Haydon PG, Oliet SH, Robitaille R, Volterra A. Gliotransmitters travel in time and space. Neuron. 2014; 81:728–739. [PubMed: 24559669]
59. Lu XM, Shear DA, Deng-Bryant Y, et al. Comprehensive evaluation of neuroprotection achieved by extended selective brain cooling therapy in a rat model of penetrating ballistic-like brain injury. Ther Hypothermia Temp Manag. 2015
60. Ohnishi M, Urasaki T, Ochiai H, et al. Selective enhancement of wnt4 expression by cyclic AMP-associated cooperation between rat central astrocytes and microglia. Biochem Biophys Res Commun. 2015; 467:367–372. [PubMed: 26431871]
61. Jelsing J, Hay-Schmidt A, Dyrby T, Hemmingsen R, Uylings HB, Pakkenberg B. The prefrontal cortex in the gottingen minipig brain defined by neural projection criteria and cytoarchitecture. Brain Res Bull. 2006; 70:322–336. [PubMed: 17027768]
62. Davidson JO, Yuill CA, Zhang FG, Wassink G, Bennet L, Gunn AJ. Extending the duration of hypothermia does not further improve white matter protection after ischemia in term-equivalent fetal sheep. Sci Rep. 2016; 6:25178. [PubMed: 27121655]
63. Martinez-Biarge M, Bregant T, Wusthoff CJ, et al. White matter and cortical injury in hypoxicischemic encephalopathy: Antecedent factors and 2-year outcome. J Pediatr. 2012; 161:799–807. [PubMed: 22682614]
64. Yang Q, Gao H, Dong R, Wu YQ. Sequential changes of endoplasmic reticulum stress and apoptosis in myocardial fibrosis of diabetes mellitus-induced rats. Mol Med Rep. 2016; 13:5037–5044. [PubMed: 27121167]

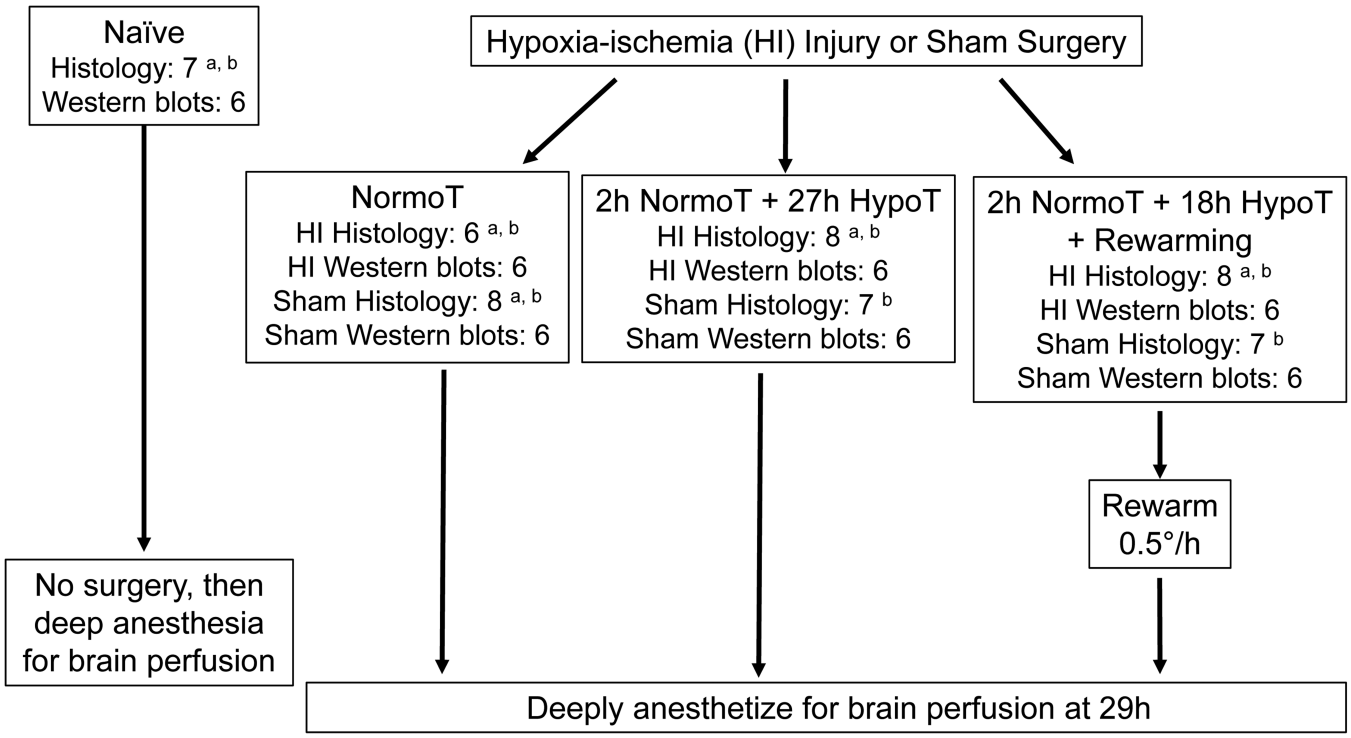

Fig 1.

Study design with randomization of piglets to hypoxic-ischemic injury or sham surgery as well as to normothermia (normoT), delayed hypothermia (hypoT), or hypothermia with rewarming. The number of piglets per group are listed. Piglet groups reported in our prior studies are denoted [4] [a] and [5] [b].

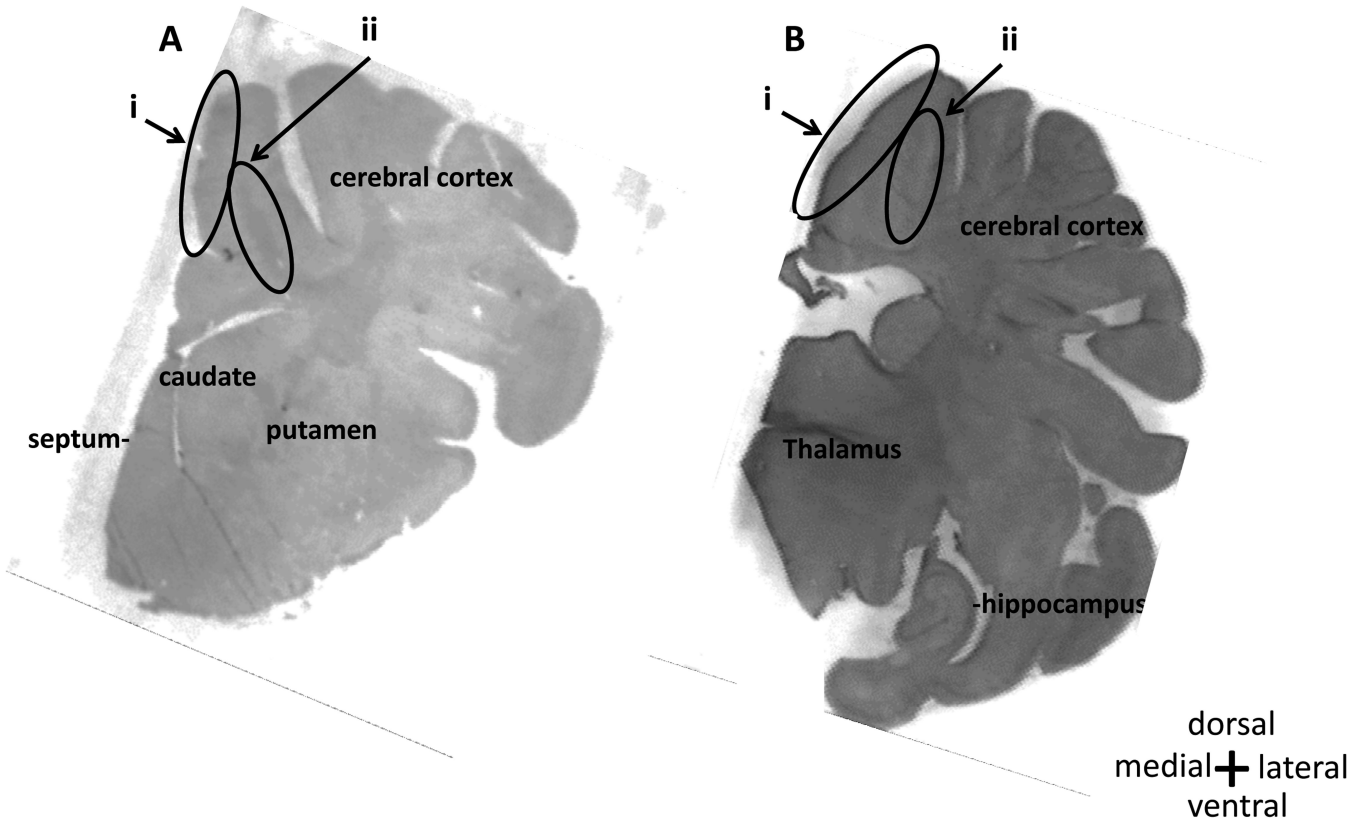

Fig 2.

Representative macrophotographs showing the anatomic regions of interest at the striatal **(A)** and hippocampal (**B**) anatomic levels. Neuronal and macroglial profiles were counted in the cortex (i) and subcortical white matter (ii) of the motor gyrus. Photographs were taken at 10X magnification; grayscale images of hematoxylin & eosin stained sections are shown.

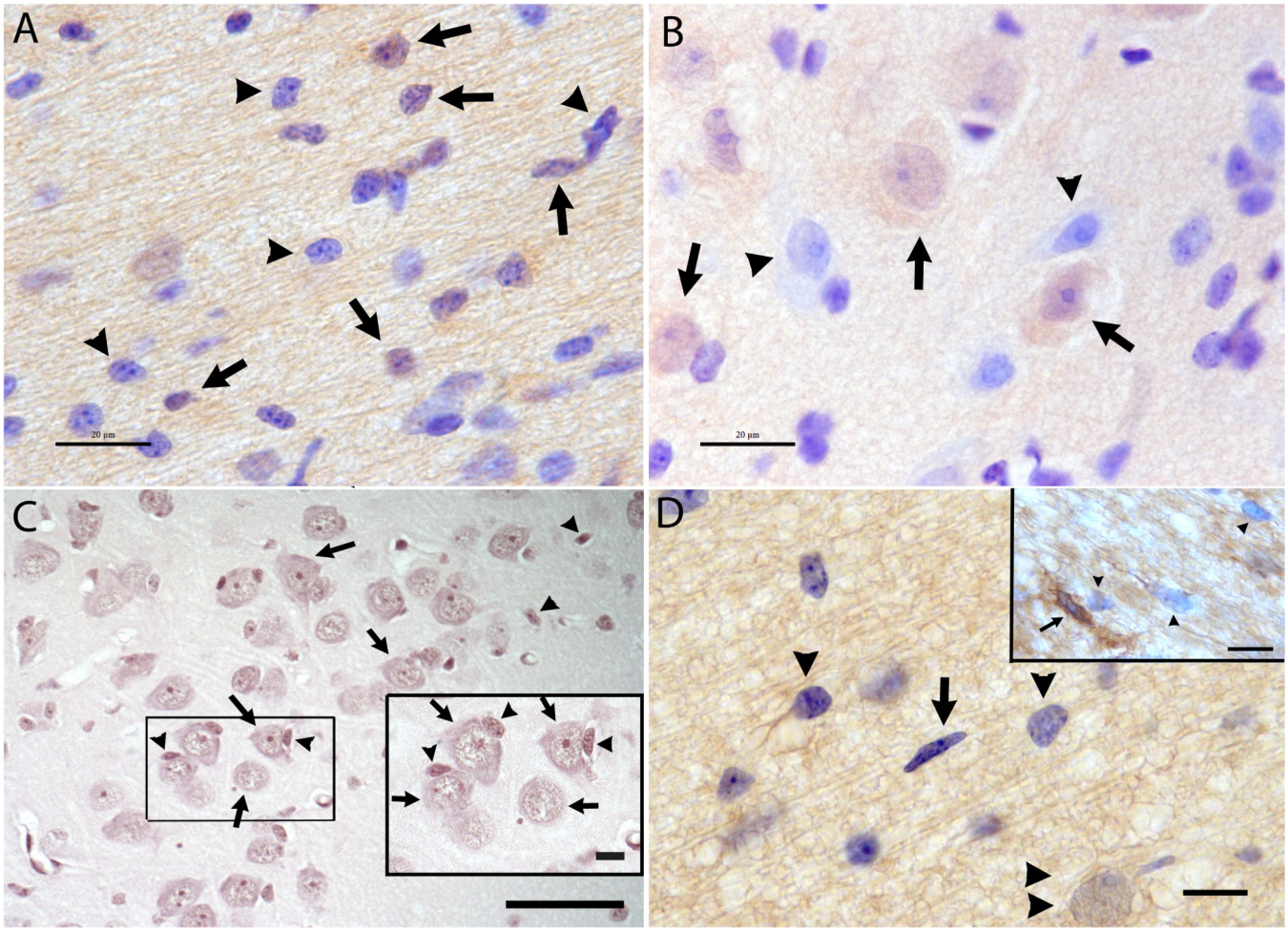

Fig 3.

Representative images show immunohistochemistry for endoplasmic reticulum to nucleus signaling 1 (ERN1) with 3,3'-diaminobenzidine substrate and cresyl violet (**A**, **B, D**); hematoxylin & eosin stain of neurons and macroglia (**C**); and immunohistochemistry for Iba-1-positive microglia with 3,3'-diaminobenzidine substrate and cresyl violet (panel **D inset**). (**A**) The subcortical white matter of the motor gyrus in a hypothermic sham piglet is shown. The arrows denote examples of ERN1+ macroglia, and the arrowheads identify examples of ERN1-negative macroglia. (**B**) Examples of ERN1+ neurons (arrows) and ERN1-negative neurons (arrowheads) in the motor cortex of a hypothermic sham piglet. (**C**) Representative images of neurons and macroglia in the motor cortex of a normothermic sham piglet illustrate the differential morphology between cell types. The arrows identify examples of neurons, distinguished by the multipolar or triangular neuronal morphology, large cell body (characteristically 8-20 μm in diameter), and open non-condensed nucleus with chromatin strands and often a nucleolus. The arrowheads show examples of the smaller macroglial cells, which include astrocytes and oligodendrocytes. Some macroglial cells are located in "satellite" positions next to the larger neurons (panel inset). (**D**) Representative images of microglia, macroglia, and neurons in the subcortical white matter of the motor gyrus in a sham hypothermic piglet. The arrow identifies a microglial cell, distinguished by

the elongated nucleus with dark chromatin. Microglia were not included in the ERN1 macroglia counts. Arrowheads denote macroglia that were counted for ERN1 immunoreactivity. The double arrowheads indicate a neuron. The inset panel shows immunohistochemistry with ionized calcium-binding adaptor molecule 1 antibody (marker for microglia), 3,3'-diaminobenzidine substrate, and cresyl violet. The arrow shows a representative microglial cell with nuclear morphology that can be differentiated from macroglia (arrowheads). Photos for panels A and B were taken at 1000X with oil immersion; the scale bars are 20 μm. The photo for panel C was taken at 400X magnification, and the scale bar is 50 μm. The inset photo for panel C was taken at 600X magnification with oil immersion, and the scale bar is 10 μm. The photos for panel D was taken at 1000X with oil immersion; the scale bar is 10 μm.

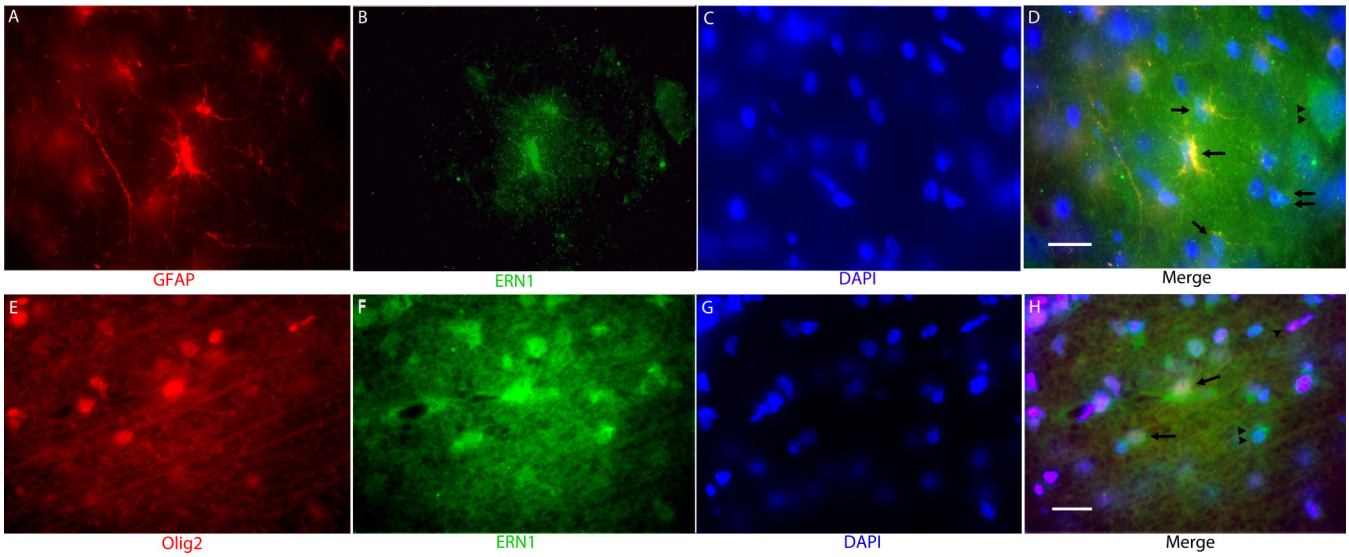

Fig. 4.

Immunofluorescent co-staining in the subcortical white matter of the motor gyrus. Panels **A–D** show glial fibrillary acidic protein (GFAP; red), endoplasmic reticulum to nucleus signaling 1 (ERN1; green) and 4',6-diamidino-2-phenylindole (DAPI; blue) in a hypothermic sham piglet. Panels **E–H** show co-staining for oligodendrocyte transcription factor (Olig2; red), ERN1 (green), and DAPI (blue) in a rewarmed sham piglet. **(D)** The single arrows denote GFAP-positive (red) astrocytes with intranuclear (blue) ERN1 (green) staining in this merged image. The double arrowheads identify a neuron that is distinguished by its large size and multipolar morphology. The double arrows show a GFAP-negative macroglial cell with intranuclear ERN1 staining. We therefore conducted additional immunostaining to identify the ERN1+, GFAP-negative cells. (**H**) The arrows identify olig2+ (red) oligodendrocytes with intranuclear (blue) ERN1 (green) staining in this merged image. The single arrowhead denotes an olig2+ oligodendrocyte that is ERN1-negative. The double arrowheads show an ERN1+ macroglial cell that is olig2-negative. Photos were taken at 1000X with oil immersion; the scale bars are 20 μm.

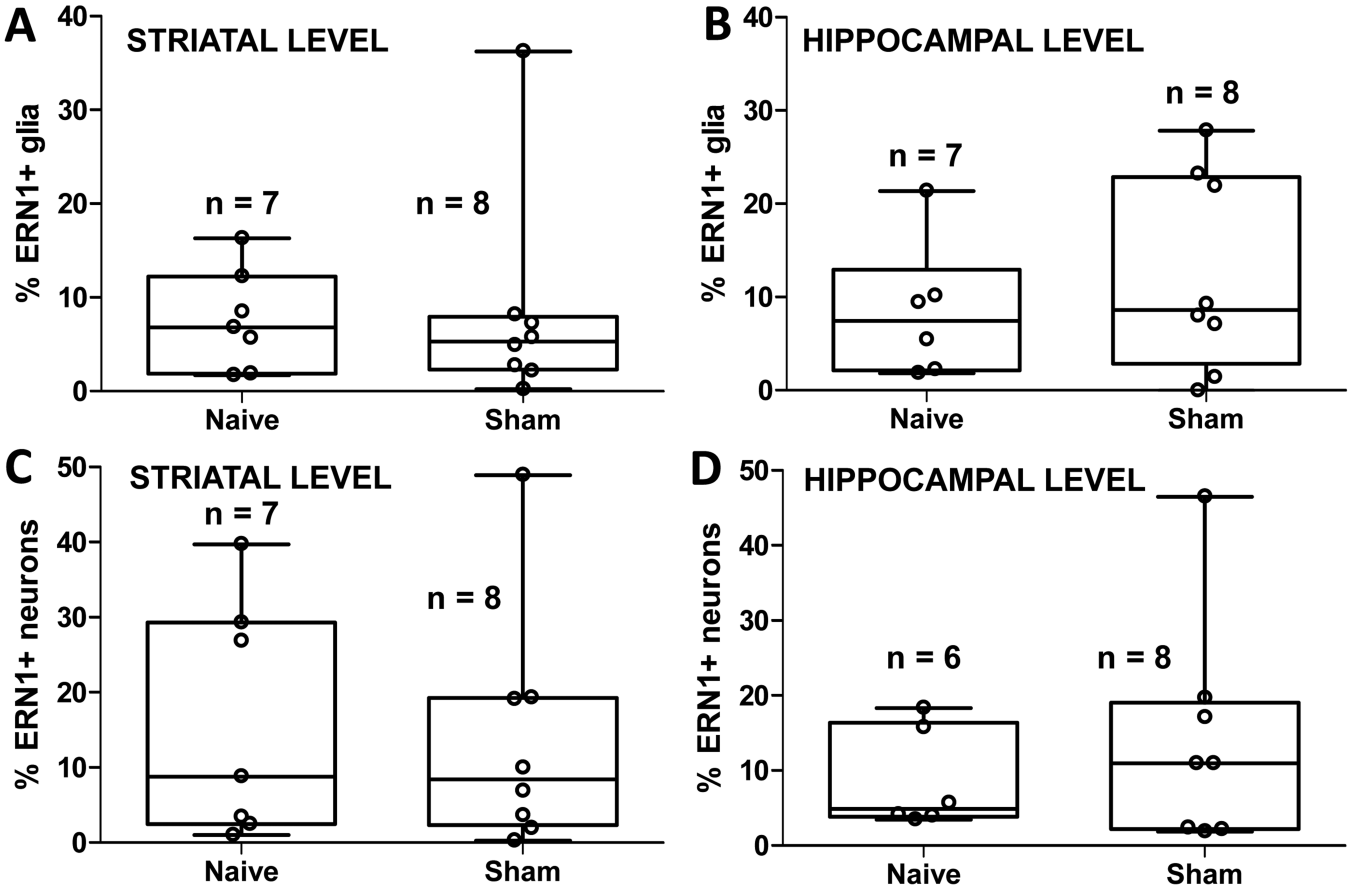

Fig 5.

The anesthetic had minimal effect on the unfolded protein response (UPR). The ratios of ERN1+ macroglia were similar in naïve unanesthetized and sham normothermic piglets at the (**A**) striatal (p=0.694) and (**B**) hippocampal levels (p=0.452). The ratios of ERN1+ neurons were also similar in naïve and sham normothermic piglets at the (**C**) striatal (p=0.867) and (**D**) hippocampal levels (p=0.950). Data were analyzed by t-tests or Mann Whitney rank sum tests. Box plots with whiskers (5^{th}-95^{th} percentiles) are shown. Each circle represents one piglet.

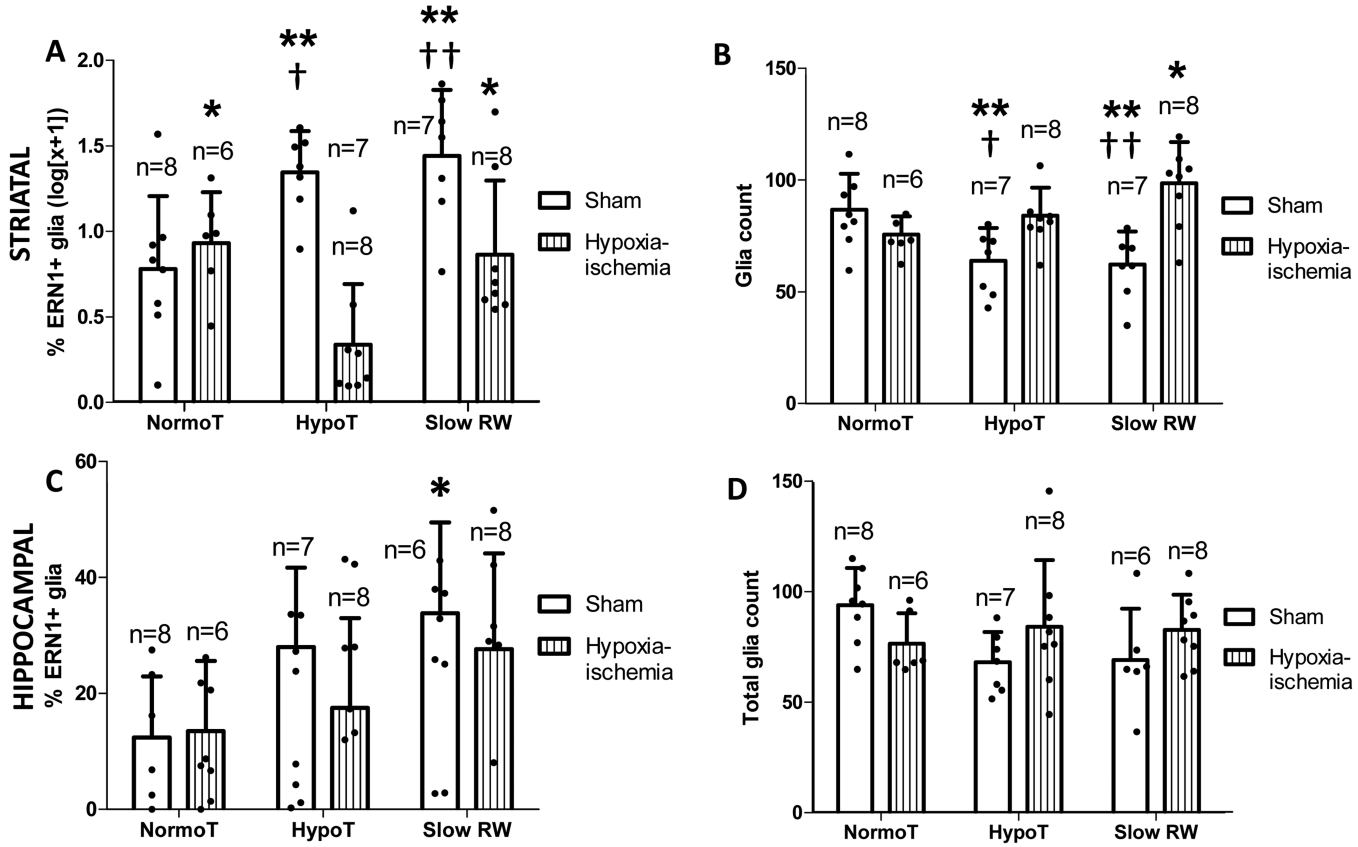

Fig 6.

ERN1+ macroglia and total macroglial cell counts in the subcortical white matter of the motor gyrus at the striatal (**A, B**) and hippocampal (**C, D**) levels. (**A**) Both hypoxia-ischemia (HI; $p<0.001$) and temperature ($p=0.046$) independently affected the ratio of ERN1+ macroglia, and there was an interaction between HI and temperature ($p<0.001$). In *post-hoc* pairwise comparisons, ERN1 expression differed among piglets that received normothermia (normoT), sustained hypothermia (hypoT), or rewarming (rewarm): *$p<0.02$ vs. HI+hypoT; **$p<0.02$ vs. sham+normoT; †$p<0.001$ vs. HI+hypoT; ††$p=0.004$ vs. HI+rewarm. (**B**) HI ($p=0.002$), but not temperature ($p=0.349$), affected the macroglial cell count. There was an interactive effect between HI and temperature on the number of macroglia ($p<0.001$). *Post-hoc* pairwise comparisons showed differences in macroglial counts: *$p=0.018$ vs. HI +normoT; **$p<0.010$ vs. sham+normoT; †$p=0.011$ vs. HI+hypoT; ††$p<0.001$ vs. HI +rewarm. (**C**) Temperature ($p=0.009$), but not hypoxia-ischemia (HI; $p=0.244$), affected the ratio of ERN1+ macroglia. When we controlled for HI, rewarming increased the ratio of ERN1+ macroglia above that during normothermia (normoT; $p=0.007$). In *post-hoc* pairwise comparisons, rewarmed shams had more ERN1+ macroglia than did normothermic shams (*$p=0.024$ vs. sham+normoT). (**D**) The macroglial cell count was not affected by HI ($p=0.516$) or temperature ($p=0.392$). Data were analyzed by 2-way ANOVA with Holm Sidak *post-hoc* pairwise comparisons. Bar graphs show means and SD. Each circle represents one pig.

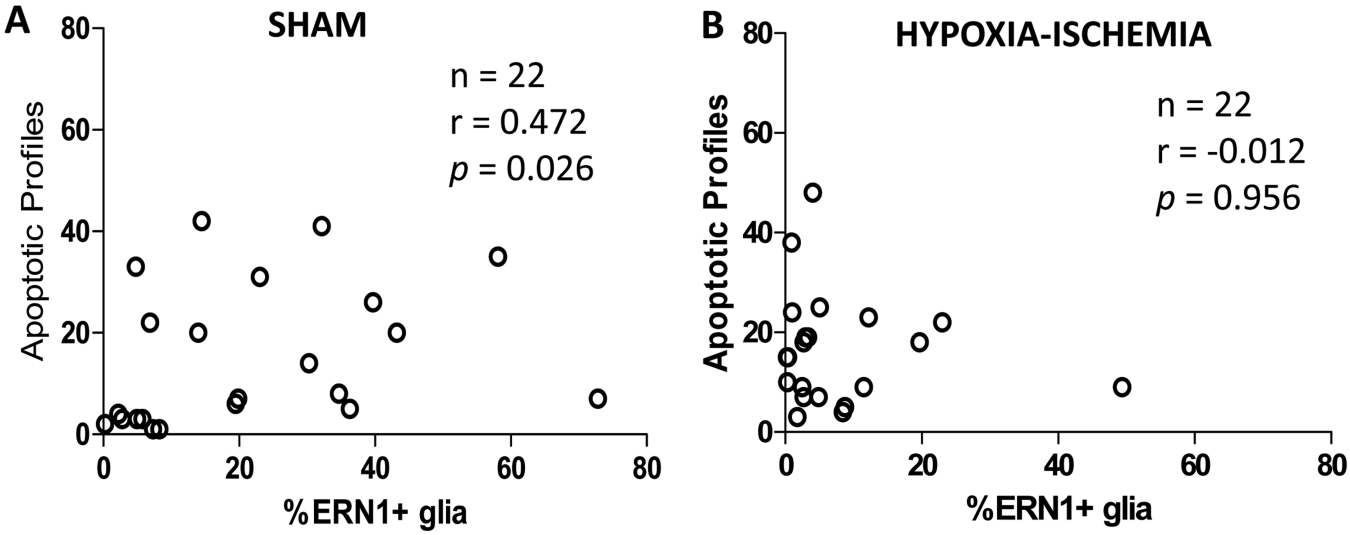

Fig 7.

Correlation between ERN1+ macroglia and apoptotic profiles in the subcortical white matter. We previously reported the macroglial apoptotic profile counts of the pigs in the current study. [5] (**A**) The ratio of ERN1+ macroglia correlated with the number of apoptotic profiles in sham (**A**) but not HI (**B**) piglets that received normothermia, hypothermia, or rewarming. Data were analyzed by Spearman correlations. Each circle represents one piglet.

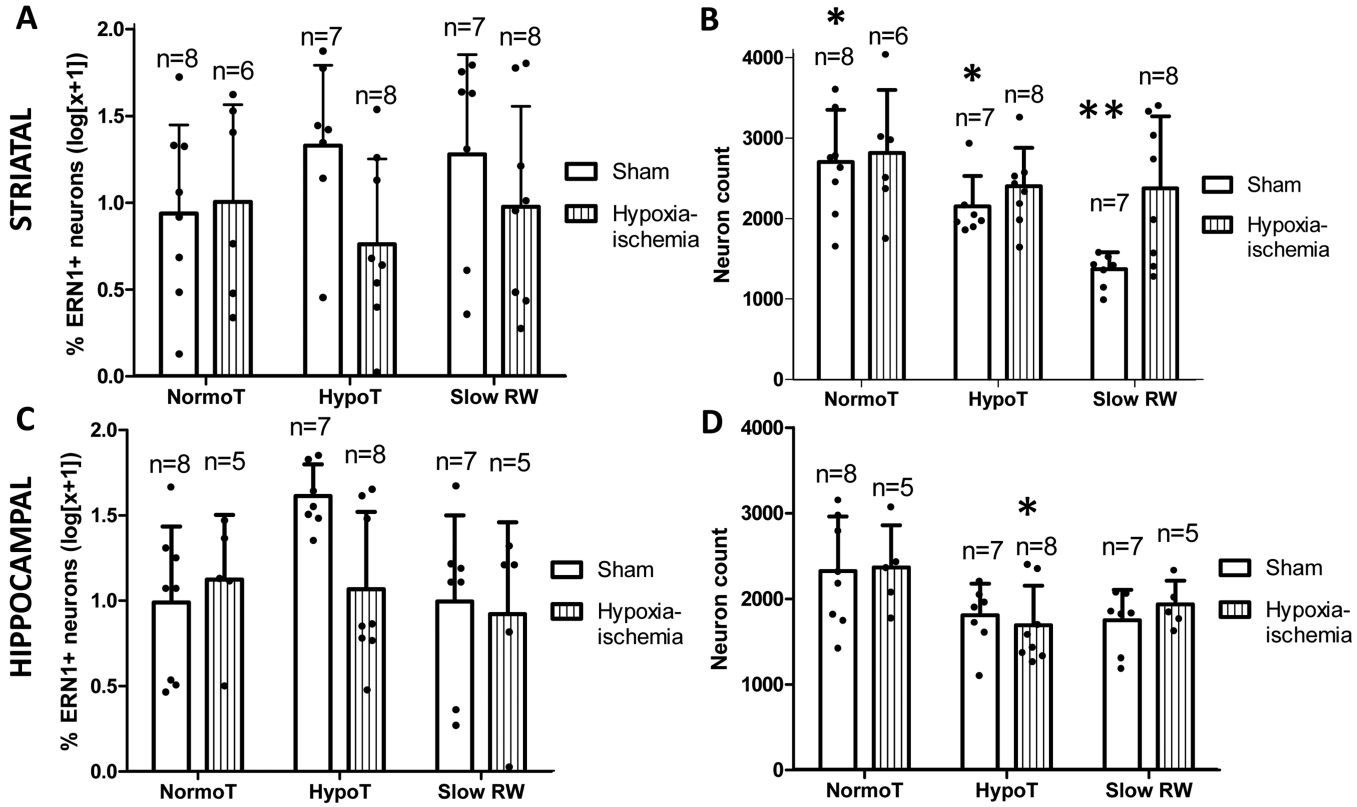

Fig 8.

ERN1+ neurons and neuronal cell counts in the motor cortex at the striatal (**A, B**) and hippocampal (**C, D**) levels. (**A**) HI (p=0.104) and temperature (p=0.738) did not affect the ratio of ERN1+ neurons. (**B**) Both HI (p=0.019) and temperature (p=0.002) independently affected the neuron count. When we controlled for HI, rewarming (rewarm) decreased the number of neurons below that observed during normothermia (normoT; p<0.001). *Post-hoc* pairwise comparisons showed differences in neuronal counts: *p<0.05 vs. sham+rewarm; **p=0.003 vs. HI+rewarm. (**C**) Neither HI (p=0.251) nor temperature (p=0.070) affected the ratio of ERN1+ neurons. (**D**) Temperature (p=0.005), but not HI (p=0.798), affected the number of neurons. When we controlled for HI, both sustained hypothermia (hypoT) and hypothermia with rewarming decreased the neuron count when compared to that with normothermia (p=0.006 for hypoT vs. normoT; p=0.022 for rewarm vs. normoT). In *post-hoc* pairwise comparisons, hypothermia decreased the number of neurons compared to that with normothermia in HI piglets (*p=0.043 vs. HI+normoT). Data were analyzed by 2-way ANOVA with Holm Sidak *post-hoc* pairwise comparisons. Bar graphs show means and SD. Each circle represents one pig.

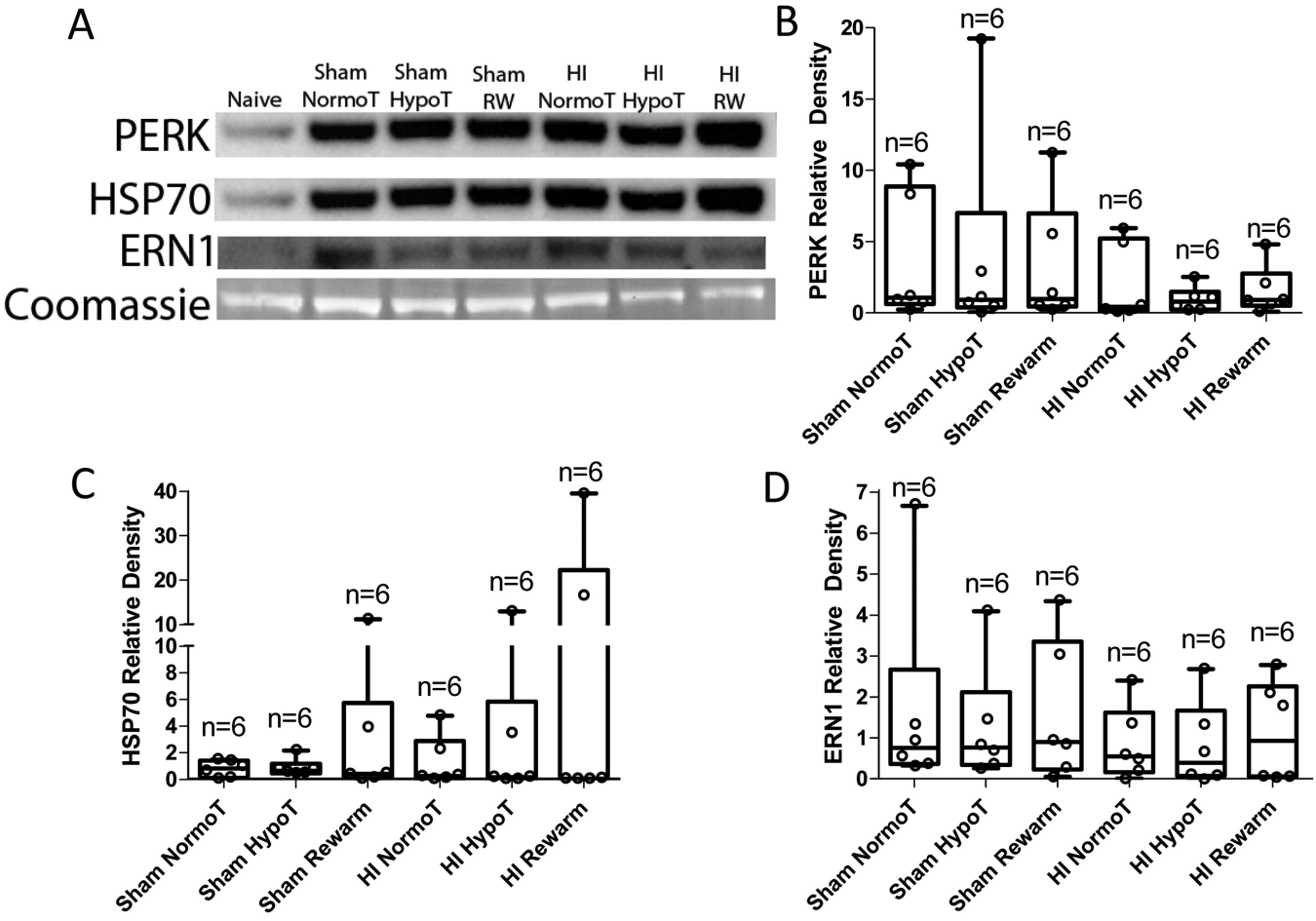

Fig 9.

Immunoreactivity of PERK, HSP70, and ERN1 in the subcortical white matter of the sensorimotor cortex. (**A**) Representative Western blots of naïve, sham+normothermia (NormoT), sham+hypothermia (HypoT), sham+rewarming (RW), hypoxia-ischemia (HI) +NormoT, HI+HypoT, and HI+RW piglets. (**B–D**) The relative densities normalized to naïve piglets were similar between groups for PERK (p=0.297), HSP70 (p=0.836), and ERN1 (p=0.345). Data were analyzed by a Friedman two-way analysis of ranks in which the four independent gels were blocked as a between-subject factor. Box plots with 5th-95th percentiles are shown. Each circle represents one piglet.

Table 1

Absolute counts of endoplasmic reticulum to nucleus signaling 1-positive (ERN1+) and total cells. Glial counts are the average of six microscope fields under 1000X magnification with oil immersion. Neuron counts are from one side of the entire motor gyrus.*

Anatomic location		Normothermia		Hypothermia		Hypothermia + rewarming	
		Sham	HI	Sham	HI	Sham	HI
Glia: striatal level	ERN1 +	4 (2, 6)	7 (5, 7)	16 (11, 22)	1 (0, 1)	26 (10, 28)	4 (3, 8)
	Total	85 (79, 96)	74 (73, 80)	69 (52, 75)	84 (80, 86)	63 (57, 71)	104 (91, 108)
Glia: hippocampal level	ERN1+	8 (4, 22)	9 (3, 18)	21 (13, 23)	13 (3, 24)	21 (14, 33)	26 (16, 33)
	Total	96 (86, 104)	69 (68, 86)	69 (57, 77)	79 (72, 91)	66 (64, 72)	83 (73, 91)
Neurons: striatal level	ERN1+	267 (86, 422)	321 (65, 733)	528 (375, 819)	88 (66, 266)	459 (149, 554)	164 (46, 455)
	Total	2732 (2388, 2973)	2780 (2440, 3049)	2000 (1956, 2138)	2417 (2163, 2573)	1439 (1274, 1498)	2395 (1553, 3150)
Neurons: hippocampal level	ERN1+	257 (44, 441)	301 (267, 405)	701 (505, 939)	121 (85, 424)	251 (84, 284)	289 (92, 316)
	Total	2273 (1816, 2871)	2387 (2098, 2458)	1918 (1680, 2023)	1517 (1368, 1878)	1847 (1576, 1978)	1861 (1783, 2037)

Abbreviations: HI, hypoxia-ischemia; IQR, interquartile range.

*Data are shown as medians (IQR).

Table 2

Endoplasmic reticulum to nucleus signaling 1-positive (ERN1+) ratios in glia and neurons*

Anatomic location	Normothermia		Hypothermia		Hypothermia + rewarming	
	Sham	HI	Sham	HI	Sham	HI
Glia: striatal level	0.05 (0.03, 0.08)	0.09 (0.06, 0.11)	0.23 (0.17, 0.31)	0.01 (0.003, 0.02)	0.35 (0.17, 0.51)	0.04 (0.03, 0.10)
Glia: hippocampal level	0.08 (0.04, 0.22)	0.09 (0.03, 0.18)	0.21 (0.13, 0.23)	0.13 (0.03, 0.24)	0.21 (0.14, 0.33)	0.26 (0.16, 0.33)
Neurons: striatal level	0.09 (0.03, 0.19)	0.14 (0.03, 0.29)	0.24 (0.16, 0.40)	0.03 (0.02, 0.13)	0.39 (0.11, 0.46)	0.08 (0.02, 0.25)
Neurons: hippocampal level	0.11 (0.02, 0.28)	0.13 (0.12, 0.23)	0.36 (0.31, 0.56)	0.06 (0.05, 0.33)	0.12 (0.06, 0.15)	0.16 (0.05, 0.16)

Abbreviations: HI, hypoxia-ischemia; IQR, interquartile range.

* Data are shown as the median ratio of ERN1+ cells (ERN1+/total cells; IQR).

Table 3

Summary of treatment effects on the unfolded protein response, apoptosis, and glial cell loss in the subcortical white matter 29 hours after hypoxia-ischemia or sham surgery.*

Treatment	ERN1+ glia ratio in white matter	Apoptosis in white matter glia	White matter total glial cell count
Striatal anatomic level			
HI + hypothermia	−	+	NS
HI + rewarming	NS	+	+
Hypothermia alone	+	+	−
Rewarming alone	+	+	−
Hippocampal anatomic level			
HI + hypothermia	NS	NS	NS
HI + rewarming	NS	NS	NS
Hypothermia alone	+	+	NS
Rewarming alone	+	+	NS

Abbreviations: HI, hypoxia-ischemia; +, increase in parameter compared to the normothermic group at $p<0.05$; −, decrease in parameter compared to the normothermic group at $p<0.05$; NS, no significant difference from the normothermic group.

*This summary is extrapolated from the current study and our past study on white matter apoptosis (Wang and Armstrong, et al., 2016). The rewarming rate is 0.5°C/hour. Data were analyzed by two-way ANOVA, and the results of *post-hoc* pairwise comparisons using the Holm Sidak method are shown. Hypothermic and rewarmed sham groups were compared to the normothermic sham group, and hypothermic and rewarmed HI groups were compared to the normothermic HI group.